

DEVELOPMENT OF ULTRASONIC CAUTERY SYSTEM

By:

YAP KAH WENG

(Matrix no.: 137872)

Supervisor:

Prof. Dr. Zaidi Mohd Ripin

July 2021

This dissertation is submitted to
Universiti Sains Malaysia
As partial fulfillment of the requirement to graduate with honors degree in
BACHELOR OF ENGINEERING (MECHANICAL ENGINEERING)




School of Mechanical Engineering
Engineering Campus
Universiti Sains Malaysia

DECLARATION

This work has not previously been accepted in substance for any degree and is not being concurrently submitted in candidature for any degree.

Signed  (YAP KAH WENG)
Date 02/07/2021

Statement 1: This journal is the result of my own investigation, except where otherwise stated. Other sources are acknowledged by giving explicit references. Bibliography/references are appended.

Signed  (YAP KAH WENG)
Date 02/07/2021

Statement 2: I hereby give consent for my journal, if accepted, to be available for photocopying and for interlibrary loan, and for the title and summary to be made available to outside organizations.

Signed  (YAP KAH WENG)
Date 02/07/2021

ACKNOWLEDGEMENT

It is a genuine pleasure in expressing my deep sense of gratitude to all the parties that have assisted me in completing this thesis. First and foremost, I would like to express my deepest gratitude to my project supervisor, Prof. Dr. Zaidi Mohd Ripin, for his guidance throughout the project. Under his professional advices and great supports, I was able to focus and complete my project successfully. His concise and precise feedbacks towards the workloads that I had presented to him had helped me to rectify mistakes and provided to me a clear research direction on the topic.

Next, I would like to thank the School of Mechanical Engineering, Universiti Sains Malaysia, and Dr. Muhammad Fauzinizam Bin Razali for providing a systematic course structure of EMD 452 Final Year Project for the fourth year students. The constant updates to the materials related to the course and preparation of webinars by Dr. Fauzi also helped me to acquire important knowledge and requirement of the course, despite the ongoing COVID-19 pandemic and online learning.

Thirdly, I would like to thank Mr. Wan Mohd Amri Wan Mamat Ali for his assistance in arranging experimental workloads. His experience in the Vibration Lab ensured that experimental work were done in the correct manner using the correct apparatus. Mr. Amri also assisted me in providing his valuable knowledge in apparatus used for experimental analysis for this project and I am grateful for his kind assistance.

Not to forget are special thanks to my senior Ph.D. student, Mr. Charvinder Singh A/L Jaginder Singh for his kind assistance in teaching me on how to correctly maneuver within the user interface of the software Abaqus. His prompt replies whenever I had a question regarding the software had helped me overcoming some of the user confusions.

Last but not least, I would like to thank my family for their unending supports that allow me to focus on my project far away from my home. Their emotional and financial supports are paramount to my success in completing this degree.

Lastly, I would, once again, express my gratitude to all parties that had directly or indirectly assisted me to complete this thesis.

TABLE OF CONTENTS

DECLARATION.....	i
ACKNOWLEDGEMENT.....	ii
TABLE OF CONTENTS	iii
LIST OF FIGURES	vi
LIST OF TABLES	ix
LIST OF ABBREVIATIONS	x
ABSTRAK	xi
ABSTRACT.....	xii
CHAPTER 1 INTRODUCTION.....	1
1.1 Overview	1
1.2 Background	1
1.3 Problem Statement	4
1.4 Project Objectives	5
1.5 Research Approach & Scope of Work	5
1.6 Thesis Outline	6
CHAPTER 2 LITERATURE REVIEW.....	8
2.1 Efficiency of Harmonic Scalpel	8
2.2 Lateral Thermal Spread and Injury	9
2.3 Commercial Cost.....	9
2.4 Theory of Piezoelectricity	10
2.5 Finite Element Modelling (FEM).....	17
2.6 Longitudinal Vibration Mode and Langevin Transducer.....	18
2.7 Other Vibration Mode	19

CHAPTER 3	RESEARCH METHODOLOGY	21
3.1	Overview	21
3.2	Simulation	22
3.3	CAD Modelling.....	23
3.4	Material Selection	25
3.5	Assembly.....	30
3.6	Interactions.....	30
3.7	Defining Analysis Steps.....	33
3.8	Load and Boundary Condition Assignments	34
3.9	Discretization of Domain	37
3.10	Solving of Solution	40
3.11	Solution Post-Processing.....	40
3.12	Experimental Analysis	40
CHAPTER 4	RESULTS AND DISCUSSIONS	44
4.1	Preloading Results.....	44
4.2	Simulated Modal Analysis	47
4.3	Simulated Harmonic Analysis.....	49
4.4	Experimental Frequency Sweep Analysis.....	50
4.5	Experimental Harmonic Analysis	50
CHAPTER 5	CONCLUSION AND FUTURE WORK	52
5.1	Conclusion	52
5.2	Future Work Recommendation	52

REFERENCES.....	54
APPENDIX A: CAD REMODEL OF PROTOTYPE.....	61
APPENDIX B: MATERIAL PROPERTIES FOR PIEZOCERAMIC MATERIAL	64
APPENDIX C: DERIVATION OF EQUATIONS FOR PIEZOCERAMIC MATERIALS	65
APPENDIX D: FIELD AND HISTORY OUTPUTs REQUESTED FOR SIMULATION	67
APPENDIX E: MISCELLANEOUS.....	69

LIST OF FIGURES

Figure 1.1: Direct and inverse magnetostrictive effects in ferromagnetic materials. (Al-Budairi, 2012)	3
Figure 1.2: (a) The direct and (b) the converse piezoelectric effects. (Safian & Soleimani, 2018).....	4
Figure 2.1: Normal and shear strains resulted from axial and shear forces. (Sharir et al., 2008)	11
Figure 2.2: Longitudinal, flexural and torsional modes.....	15
Figure 2.3: Simple lumped mechanical model for a Langevin transducer. (PiezoDrive, n.d.)	16
Figure 3.1: Overview diagram of solutions.	21
Figure 3.2: Existing ultrasonic scalpel.....	23
Figure 3.3: Assigning sections.....	29
Figure 3.4: Material orientation assigned for piezoceramic ring.....	30
Figure 3.5: Assembly of parts and constraints used.	30
Figure 3.6: Tangential behaviour of General Contact interaction.	31
Figure 3.7: Normal behaviour of General Contact interaction.	31
Figure 3.8: Propagation of interaction to future analysis steps.....	32
Figure 3.9: Tie constraint for front mass-back mass surface pair.....	33
Figure 3.10: Tie constraint for front mass-cutting tool surface pair.....	33
Figure 3.11: All analysis steps with <i>Nlgeom</i> turned on to account for non-linearity effects.....	34
Figure 3.12: Preload applied using the Bolt Load module with a force of 3700 N...	35
Figure 3.13: Arbitrary <i>Encastre</i> boundary condition for preloading.....	35
Figure 3.14: Zero electric potential BC on piezoceramic rings.....	36

Figure 3.15: BC applied for harmonic analysis.	37
Figure 3.16: Meshed assembly.	37
Figure 3.17: Mesh element type for non-piezoelectric parts.	39
Figure 3.18: Mesh element type for piezoelectric part.	40
Figure 3.19: Full experimental set-up.	41
Figure 3.20: Scalpel with manufactured casing secured using a mechanical jig.	41
Figure 3.22: Keyence laser system used.	42
Figure 3.23: Measuring system display.	42
Figure 3.24: NI compactDAQ.	42
Figure 3.21: Sinusoidal input voltage with $300V_{pp}$	43
Figure 4.1: Stress contour after preloading.	44
Figure 4.2: Stress contour with a 100-scale factor.	44
Figure 4.3: Nodes selected for stress values.	45
Figure 4.4: Stress applied on piezoceramic ring due to preloading.	45
Figure 4.5: Node selected at the centre of the bolt section.	46
Figure 4.6: Resultant stress in bolt after preloading.	47
Figure 4.7: Resonant frequency of 47740 Hz with a dominantly longitudinal mode shape.	47
Figure 4.8: Comparison between deformed and undeform models.	48
Figure 4.9: Path along the length of model created in post-processing.	48
Figure 4.10: Relative displacement in Z-direction along the length of model.	48
Figure 4.11: Simulated mechanical response at the tip of the ultrasonic horn due to harmonic excitation.	49
Figure 4.12: Resonance frequencies detected in the range of 40 kHz to 50 kHz.	50

Figure 4.13: Mechanical response of tool-tip under harmonic excitation (time domain)
..... 51

LIST OF TABLES

Table 2.1: Different types of piezoelectric charge constants.....	11
Table 3.1: Parts and their functions.	23
Table 3.2: Mechanical properties of stainless steel used (AZoM, 2012).....	26
Table 3.3: Mechanical properties of aluminium alloy used (MatWeb, n.d.-a).....	26
Table 3.4: Mechanical properties of copper alloy used (MatWeb, n.d.-b)	27
Table 3.5: Manufacturer provided data for piezoelectric material used (CeramTech, n.d.)	27
Table 3.6: Piezoelectric properties of piezoceramic ring.....	28
Table 3.7: Master and slave surfaces for tie constraints	32
Table 3.8: Meshing details for each part.....	38
Table 4.1: Average stress magnitude imposed on the surface of the piezoceramic ring.	46

LIST OF ABBREVIATIONS

1D	One-dimensional
2D	Two-dimensional
3D	Three-dimensional
AECUSM	Animal Ethics Committee of USM
AI	Artificial intelligence
BaTiO ₃	Barium titanate
BC	Boundary condition
BT	Barium titanate
CAD	Computer-aided design
CAE	Computer-aided engineering
DAQ	Data Acquisition
D.O.F	Degree of freedom
EBL	Estimated blood loss
EBVS	Electro-thermal bipolar vessel sealing
EMA	Experimental modal analysis
FEA	Finite element analysis
FEM	Finite element modelling
HS	Harmonic scalpel
INR	Indian Rupee
IUVAS	Integrated ultrasonic variable amplitude system
JEPeM	Jabatan Etika Penyelidikan (Manusia)
MATLAB	Matrix Laboratory
ML	Machine learning
ODB	Output database
OR	Operating room
PZT	Lead zirconate titanate
SAE	Society of Automotive Engineers
USM	Universiti Sains Malaysia

ABSTRAK

Penggunaan elemen piezoelektrik dalam penjaan getaran dalam transduser ultrasonik telah menjadi sesuatu yang biasa dalam perkembangan sistem cauteri ultrasonik. Cara untuk mencirikan sesuatu skalpel ultrasonik yang betul telah merupakan sesuatu proses reka bentuk yang penting. Dalam kajian ini, sesuatu prototaip skalpel harmonik telah dicari menggunakan pemodelan elemen terhingga dan prosedur eksperimen. Perisian Abaqus telah dipakai untuk mengkaji kesan pramuat, bentuk mod membujur yang betul, frekuensi resonan dan tindak balas mekanikal ekoran pengujaan harmonic. Analisis kaedah eksperimental modal dan harmonik digunakan untuk pengesahan keputusan. Keputusan daripada simulasi adalah hampir seiri dengan kiraan teori untuk kesan pramuat, di mana tekanan mampatan bernilai 27 MPa yang mencukupi telah dikenakan ke atas bahagian piezoceramic. Tekanan dalaman yang diwujudkan dalam bahagian bolt mencapai 190 MPa. Analisis modal mengesan satu frekuensi resonan bernilai 47740 Hz dengan bentuk mod membujur. Bagi analisis harmonik, hasil simulasi merekodkan amplitud tindak balas mekanikal sebanyak 76.85 mikron manakala prosedur eksperimen merekodkan 54 mikron. Hasil kajian menyimpulkan bahawa process pencirian skalpel ultrasonik adalah berjaya.

ABSTRACT

The use of piezoelectric element as the primary ultrasonic transducer is prevalent in ultrasonic cautery system. Proper method to characterize an ultrasonic scalpel has become an important design process. In this study, an ultrasonic scalpel prototype was characterized using both finite element modelling and experimental procedures. FEM simulation software, Abaqus was utilized to investigate preloading effects, proper longitudinal mode shape, resonant frequency, and mechanical response due to harmonic excitation. Experimental modal and harmonic analyses were used for experimental validation. The simulated results were in accordance to the theoretical calculation for the preloading effects, where sufficient compressive stress of 27 MPa was imposed onto the piezoceramic rings and an internal stress developed within the bolt approached 190 MPa. Modal analysis detected a resonant frequency at 47740 Hz with a dominant longitudinal mode shape. For harmonic analysis, simulated result suggested 76.85 microns of mechanical displacement amplitude while experimental procedure measured 54 microns. The results concluded that the ultrasonic scalpel was successfully characterized.

CHAPTER 1

INTRODUCTION

1.1 Overview

This chapter covers the research background, the problem statement, the research objectives, the research approaches taken, the research scope, and the thesis outline of this study. The background of the ultrasonic scalpel and its working principle and applications provide a basic framework for the research work. The problem statement has pointed out the problems faced in this study. There are several research objectives needed to be achieved in this study. The research approaches taken and the research scope clarified are used to ensure that the research objectives are achieved. Lastly, the overall thesis outline of this study is summarized.

1.2 Background

1.2.1 Medical Engineering and Technology

Due to rapid advance in medical technology, in the last decade, increasing number of engineering technologies are developed and applied in different medical fields and have shown significant improvements. Two of the most common examples would be the use of 3D printing in generating biocompatible medical structures (Li et al., 2021) and the use of machine learning (ML) and artificial intelligence (AI) in diagnosis of medical problems (Syaifullah et al., 2021). Another prominent example of engineering technology employed recently was the use of 3D printing of medical ventilator filter (Shaylor et al., 2021), which greatly reduces the cost and enhances the productivity and velocity of producing these life-saving equipment.

In the surgical field, which is the domain of this study, engineering is also utilized to improve the efficiency and efficacy of surgical processes. In minimally-invasive surgeries (Ochsner, 2000) such as laparoscopy and invasive surgeries (Cousins et al., 2019) such as any form of skin incision, the use of tissue-cutting devices known as scalpels are essential. Before the introduction of ultrasonic cautery procedures, the use of traditional

electrocautery systems such as monopolar and bipolar cautery systems are prevalent. Since its invention, the ultrasonic cautery system has been deployed and utilized in various types of surgeries in an increasing rate due to its better performance in terms of cutting speed, lateral thermal spread reduction and post-operative recovery, which are proven in multiple research papers included in the next chapter.

1.2.2 Working Principle of Ultrasonic Cautery

The working principle of an ultrasonic cautery system is briefly introduced here. Ultrasonic cautery system works on the principle of protein denaturation. When applied to soft tissues, the ultrasonic scalpel transfer the mechanical energy from the device to the tissue in the form of friction. Heat produced through friction raises the temperature of the protein and breaks the hydrogen bonds within the tissue and transforms it into an adhesive material named coagulum to seal the vessels (Amaral, 1994). Hence, using an ultrasonic scalpel allows simultaneous cutting and coagulating, hence minimizing blood loss and simplifying surgery steps as no additional equipment is needed to initiate haemostasis process. The heat produced by ultrasonic cauterizing is far lower than that of electrocautery systems and no electricity flows through the patient. Lower heat leads to lower temperature at the site of dissection hence lower lateral thermal injury and less charring. Ultrasonic scalpel also produces less smoke and allows better visibility during operations. In the next chapter, various research papers focusing on the study in viability of ultrasonic cautery system and comparison with other similar cautery systems are included in details.

1.2.3 Ultrasonic Transducer and Wave Generation Methods

At the heart of an ultrasonic cautery device, the ultrasonic transducer is an integral part of the device. A transducer can be defined as a component that converts one form of energy to another (Agarwal, 2005). For an ultrasonic transducer, electrical energy is converted into mechanical energy. The term ultrasonic indicates that the mechanical energy, in the form of sound and/or vibration, is in the ultrasonic range with a frequency higher than the upper acoustic threshold for human hearing at 20,000 Hz. Most ultrasonic power transducers work in the range of 20 to 100 kHz (Gallego-Juarez, 1991). Frequencies higher than 100 kHz (up to few GHz) are used for non-destructive testing and inspections

(IOlympus, 2006). For medical-use ultrasonic scalpel, commercial products are designed to work at around 55,000 kHz (Dutta & Dutta, 2016).

In ultrasonic power transduction, three of the most common methods used to generate ultrasonic mechanical energy are through the use of the Galton’s whistle, the magnetostrictive effect and the inverse piezoelectric effect (Al-Budairi, 2012). For the Galton’s whistle, ultrasonic waves are generated in fluids passing through a resonance cavity or a reflector producing fluids with ultrasonic characteristics. The whistle was invented by Sir Francis Galton (1822-1911) and he had recorded most of his efforts in producing the animal-hearing testing device in his 1883 book “*Inquiries into Human Faculty and Its Development*” (Joyce & Baker, 2011).

For magnetostrictive effect, ferromagnetic materials are exposed to an external magnetic field and the material will expand and contract. As a magnetic field is applied to the material, its molecular dipoles and magnetic field boundaries rotate to align with the field. This causes the material to strain and elongate (Ekreem et al., 2007). The effect was first measured by James Prescott Joule (1818-1889) who was able to magnetize a nickel sample and measure the change in length in the sample (Garcia & Elsheikhi, 2016). The reciprocal effect, in which the applied magnetic field is changed due to a mechanical forces is called the Villari effect (Riesgo et al., 2020). Both magnetostrictive and Villari effects are out of the scope of this study hence the details of energy transduction are omitted.

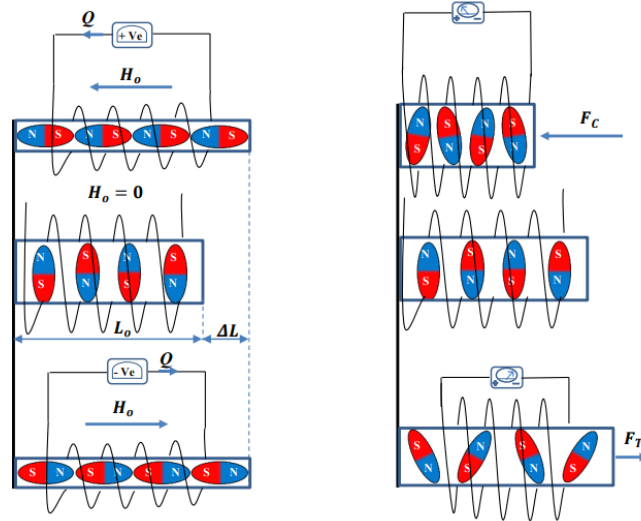


Figure 1.1: Direct and inverse magnetostrictive effects in ferromagnetic materials. (Al-Budairi, 2012)

Apart from the two methods discussed, piezoelectricity is another common method used to generate ultrasonic waves. The word ‘piezo’ in piezoelectricity came from the Greek word ‘*piezien*’, which means ‘to squeeze or presses’. Piezoelectricity is a material property found in certain materials, in which an electric field will be generated when it is subjected to external mechanical forces, either tensile or compressive. This effect is known as the direct piezoelectric effect, first discovered by the Curie Brothers in 1880 (Manbachi & Cobbold, 2011). The inverse of the effect is also true, where the application of an external electric field through a potential difference will generate mechanical stresses and strains in certain materials, which is known as the converse piezoelectric effect, first discovered by Gabriel Lippmann through mathematical derivation from the thermodynamics principles in 1881 (Al-Budairi, 2012; Uchino, 2010). When the polarity of the electric field constantly reverses direction, the piezoelectric material will experience elongation and compression. When the rate of reversal is high, ultrasonic wave can be generated from the rapid deformation of the material. Piezoelectricity can be found in natural materials such as quartz and Rochelle salts, and man-made materials such as Barium Titanate (BaTiO_3 , BT) and Lead Zirconate Titanate (PZT) (Uchino, 2010). Due to better characteristics of the converse piezoelectric effect compared to the magnetostrictive effect (Al-Budairi, 2012), the converse piezoelectric effect is chosen as method for ultrasonic transducer design for this project.

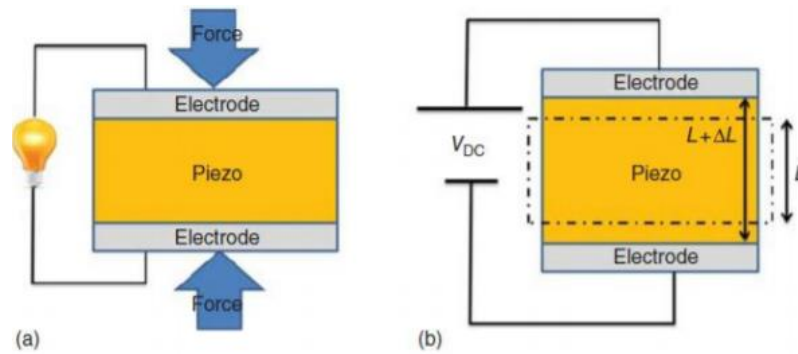


Figure 1.2: (a) The direct and (b) the converse piezoelectric effects. (Safian & Soleimani, 2018)

1.3 Problem Statement

A large number of professional studies performed comparing the uses of traditional electrocautery with ultrasonic, or commonly known as harmonic cautery have suggested

that the latter has significant medical advantages, which generally include lower thermal injury, better haemostasis, decrease blood loss and better postoperative recovery. Hence, there exists an encouraging motivation to develop stronger ultrasonic cautery systems. In order to determine the degree of effectiveness of the system, or in simpler words, how strong is an ultrasonic cautery system, a systematic system that is capable of characterizing the performance of the scalpel designed is therefore required. Therefore, the main objective of this project is to focus on characterizing an existing ultrasonic scalpel prototype using suitable methods. The tested performance outputs are mode shapes, natural frequencies, harmonic-excited mechanical displacement, and electrical impedance and phase angles. The methods used are finite element modelling (FEM) and experimental modal analysis (EMA) in the Vibration Lab.

1.4 Project Objectives

- 1) To carry out finite element analysis of a coupled piezoelectric and structured simulation simulated under voltage excitation.
- 2) To carry out modal analysis of the scalpel using FEM.
- 3) To measure the displacement of the tip of the prototype under voltage excitation through simulation and experiment.

1.5 Research Approach & Scope of Work

The research approach taken and the scope of work can be roughly classified into three different sections across the entire project's duration, which are literature review and background research, computer-aided design (CAD) and finite element modelling (FEM), as well as experimental modal analysis and validation. The details of each section are briefly discussed as followed.

1.5.1 Literature Review & Background Research

As with all other research project, the project begins with a literature review and background research to determine the amount of researches conducted by others in the related field. Background research is conducted to investigate the concept of ultrasonic

scalpel, ultrasonic transducer and piezoelectric materials. In this part of the research, efforts are also allocated in determining the proper platform used for FEM and designing the experimental modal analysis and validation procedures. The literature review, which will be discussed in details in the next chapter, focuses on research and journal papers on medical evaluation of efficiency and efficacy of ultrasonic cautery system compared to other competitors, cost evaluation of ultrasonic scalpels, finite element modelling (FEM) and finite modelling analysis (FEA) done by other researchers in modelling ultrasonic transducer systems, and potential ultrasonic transducers working in other mode of vibrations such as flexion, torsion and combined modes. The literature review is a continuous process conducted until the end of the project.

1.5.2 Computer-Aided Design and Finite Element Modelling

In this part of the project, CAD is used to remodel the ultrasonic scalpel. FEM is conducted to simulate the entire ultrasonic scalpel in order to conduct modal analysis for natural frequency and mode shape, and dynamic analysis to determine the steady state response of the system in terms of tip displacement amplitude.

1.5.3 Experimental Analysis & Validation

After simulation is done, the scalpel is characterized using experimental analysis to determine the actual resonance frequency of the system. Experimental method is employed to determine the actual stroke length achievable using the scalpel utilizing laser measuring system and external piezo-driving apparatus. Validation is performed to cross-check with the results obtained from simulations. Experimental procedures involved are detailed in Chapter 3: Research Methodology.

1.6 Thesis Outline

The structure of this thesis is outlined in this section. The thesis starts with a declaration and acknowledgement. It is followed by a table of content and comprehensive lists of figures, tables and abbreviations used. Next, an abstract is prepared to briefly summarize the main features of the project. It is then written into five distinctive chapters, which are the introduction, the literature review, the research methodology, the results and

discussions and finally followed by the conclusion and any recommended future work. The thesis is ended with a list of references and appendices.

CHAPTER 2

LITERATURE REVIEW

2.1 Efficiency of Harmonic Scalpel

Ultrasonic cautery systems have been widely compared with traditional cautery systems such as monopolar, bipolar and other types of electrocautery systems. Mathialagan et al. (2016) confirmed that shoulder pain was significantly lesser for harmonic scalpel patient group compared to the electrocautery patient group, and greater improvement in post-operative shoulder movement following neck dissection. Mittal et al. (2017) had shown that harmonic scalpel use in modified radical mastectomy provided significant reduction in intraoperative blood loss, better haemostasis and more effective lymphatic vessels occlusion. Arvind et al. (2018) also concluded that there was lesser intraoperative estimated blood loss (140.8 mL) for harmonic cautery compared to electrocautery (182.6 mL). In the same research, it also found that the operative time is shorter for harmonic cautery (141 minutes) compared to electrocautery system (197 minutes).

A meta-analysis in harmonic scalpel versus electrocautery for parotidectomy confirmed shorter surgical time, less intraoperative blood loss, shorter hospital stays and lower incidence of transient facial nerve paralysis for the former in nine research papers (D. Li et al., 2019). A pilot study in tonsillectomy safety and patient satisfaction between using HARMONIC ACE® and monopolar diathermy also confirmed less intraoperative bleeding, lower risk of delayed haemorrhage, earlier return to normal diet and activities and better visibility in surgical field due to less bleeding and smoke (Kwek et al., 2020). Patients utilizing harmonic scalpel has significant shorter mean drainage duration and total drainage volume in post-operative recovery of capsulectomy at the second stage of expander/implant breast reconstruction, which suggest better post-operative recovery (Kim et al., 2020). Comparison points in all six-research papers mentioned are common in the scope of intraoperative estimated blood loss (EBL), post-operative recovery and intraoperative time. Ultrasonic cautery systems generally score better in these three criteria suggesting it is competitively viable in certain surgeries compared to electrocautery systems.

2.2 Lateral Thermal Spread and Injury

Despite the advantages provided, ultrasonic cautery still poses a common problem found in most cautery systems, which is lateral thermal spread and injury. One example of lateral thermal injury in electrocautery system is thermal spread of more than 2cm laterally from the dissection site with significant temperature rise recorded using real-time infrared thermography, resulted in perforation and necrosis (Nechay et al., 2020). This shows that lateral thermal injury in traditional electrocautery system is highly unfavourable and in need of better alternatives. Harmonic scalpel recorded lower peak temperature and temperature rise than bipolar electrocautery and its performance is comparable to the hybrid system of electro thermal bipolar vessel sealing system (EBVS), however both EBVS and HS are considered valid and safe devices for ear, nose and throat surgeries (ENT) (Tirelli et al., 2015).

Comparison of lateral thermal spread of four common energy sources used for cautery systems using a porcine model showed that ultrasonic cautery system caused lower ovarian tissue thermal injury (0.41 ± 0.27 mm) compared to monopolar electrocautery (0.99 ± 0.82 mm). Lower uterine tissue thermal injury (0.48 ± 0.2 mm) compared to bipolar instruments (1.15 ± 0.2 mm) is also recorded and comparable to plasma energy method, which has the lowest thermal spread among the four sources (Llarena et al., 2019). Hence, there are adequate evidences that point to the fact that ultrasonic cautery is a better option than most electrocautery systems in the context of minimizing lateral thermal spread and injuries.

2.3 Commercial Cost

Another factor of concern for ultrasonic cautery system is the cost factor. Harmonic scalpel surgeries cost an additional 33,000 INR compared to electrocautery surgeries in India (Arvind et al., 2018). This shows a serious medical and economical disadvantage as the importance of fiscal responsibility rests heavily on physicians in developing countries like India. Other research papers also showed the higher cost of the use of ultrasonic cautery systems, but provided arguments stated that the cost is balanced by the improved surgical efficiency and patient post recovery. The higher cost of using harmonic scalpels is balanced

by the lower cost of needed blood products such as analogous pre-donated fresh frozen plasma and red blood cells due to significant lower intraoperative estimated blood loss (Cakir et al., 2006). Shorter OR time and improved clinical outcomes in a variety of procedures resulted in the higher device cost are offset by increase in surgical efficiency (Hsiao et al., 2015). Usage of Harmonic devices resulted in a significant 8.7% reduction in procedure costs or roughly 228 USD per procedure in favour of the Harmonic devices and the high device cost may be offset by the reduction in costs for surgical procedure and hospital resources used (Cheng et al., 2018). These research papers form a strong basis in this project to design and develop a more cost-effective ultrasonic cautery system.

2.4 Theory of Piezoelectricity

The generic background to the use of piezoelectricity in the generation of acoustic waves and the transduction of electrical to mechanical energy in ultrasonic transducers are mentioned in the previous chapter. In this subsection, the theory of converse piezoelectric effect and related formulations are investigated and summarized. The direct piezoelectric effect, where the application of mechanical energy to electrical energy, despite similar (in fact, reciprocal) in terms of the working principle and physics involved, will be omitted in this part of the discussion.

2.4.1 Piezoelectric Constitutive Equations

In linear elasticity theory, for isotropic, non-piezoelectric materials, under elastic condition where the material reverts back to its original dimensions without plastic deformation, the application of axial stress, σ will produce an equivalent strain, ϵ and shear stress, τ will produce an equivalent shear strain, γ , related by the elastic modulus, E and the shear modulus, G respectively as shown as followed (Mase et al., 2020):

$$\sigma = E \cdot \epsilon \quad (1)$$

$$\tau = G \cdot \gamma \quad (2)$$

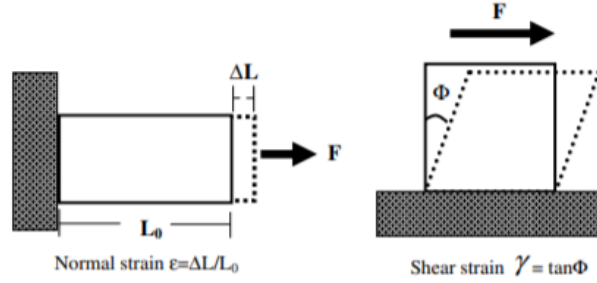


Figure 2.1: Normal and shear strains resulted from axial and shear forces.
(Sharir et al., 2008)

The elastic and shear moduli are also related through the following formulation:

$$E = 2G(1 + \nu) \quad (3)$$

Where ν is the Poisson's ratio of the material.

For anisotropic piezoelectric material, material strain can also be induced from an external electrical field, E , where the magnitude of the induced strain is defined as followed:

$$S = d_{ij} \cdot E \quad (4)$$

Where d is defined as the piezoelectric charge constant of the material. The constant is normally denoted in the form of d_{ij} , where i is the direction of polling of the material, and j is the direction of the piezoelectric-induced strain. There are three types of common piezoelectric charge constants depending on the direction of polling and induced strain, which are shown in the following table:

Table 2.1: Different types of piezoelectric charge constants.

Constant	Polling Direction	Induced Strain Direction	Direction Reference
d_{31}	3	1	
d_{33}	3	3	
d_{15}	1	5 (Shear strain)	

For ultrasonic transducers utilizing longitudinal vibration mode, the polling direction and the induced strain direction are parallel and in the thickness direction, and the constant is commonly denoted in the form of d_{33} . The constant has a unit of Coulomb per unit Newton (C/N). The magnitude of the charge constant is usually very small, which is in the pico-range. High piezoelectric charge constant is desired for materials designed for motion or vibration generation, such as ultrasonic actuators (Liu, 2001).

At low electric field, the piezoelectric effects can be modelled in the form of linear constitutive equations, where the dependency of both effects (direct and converse) on the piezoelectricity charge constant, elasticity and electrical boundary conditions are defined accurately. The most common form of the piezoelectric constitutive equation, in the Strain-Charge form, is shown as followed (Liu, 2001):

$$D = d \cdot T + \epsilon^S \cdot E \quad (5)$$

$$S = s^E \cdot T + [d]^t \cdot E \quad (6)$$

Where the notations used are defined as followed:

D	: Electric displacement
T	: Mechanical stress
ϵ^T	: Absolute permittivity of free space at constant strain
E	: Electric field
S	: Mechanical Strain
s^E	: Elastic compliance (reciprocal of the elastic modulus)
d	: Piezoelectric charge constant (superscript t indicates transpose)

Equation (5) can be seen in direct piezoelectric effect where the application of force-manifested stress causes a change in electrical displacement. Equation (6) shows that electrical strain is induced by the introduction of an external electric field. Piezoelectric charge constants are present in both equations, indicating that piezoelectric materials exhibit both effects. The linear constitutive equations can only be applied when the piezoelectric effects are considered linear. In real life applications, piezoelectric effect is non-linear and is affected by hysteresis and creep (Muhammad et al., 2015; Sabarianand et

al., 2020). The piezoelectric constants are also depended on the temperature and the electric field.

The piezoelectric constitutive equations can also be written in tensor notations. Tensor notations are generally applied to solve mathematical and physical problems such as tensor calculus and mechanics problems. In an m-dimensional space, a rank-n tensor is a mathematical object that has n indices, m^n components that obeys certain transformation rules. Scalars and vectors are some example of tensors. For example, a 0th order tensor (E.g. Density) has $3^0 = 1$ component, which is the magnitude, while a 1st order tensor (E.g. Displacement), has $3^1 = 3$ components in the 3-dimensional vector space (i, j, k vector notations) (Faculty of Khan, 2018). Another reason to use tensor notation is that the software Abaqus used for FEM also utilizes tensor notations inputs such as elastic modulus of piezoelectric materials. The linear constitutive equations, when written in the tensor notation, are shown as followed (Characterization, 1998):

$$D_i = d_{ikl} \cdot T_{kl} + \varepsilon_{ik}^S \cdot E_k \quad (7)$$

$$S_{ij} = s_{ijkl}^E \cdot T_{kl} + [d_{ikl}]^t \cdot E_k \quad (8)$$

Based on the symmetry of the tensors used, the piezoelectric constitutive equations can also be written in a compact matrix form as followed:

$$\begin{Bmatrix} D \\ S \end{Bmatrix} = \begin{bmatrix} d & \varepsilon^S \\ s^E & d^t \end{bmatrix} \begin{Bmatrix} T \\ E \end{Bmatrix} \quad (9)$$

Equation 9 can be written in an expanded-matrices form as shown as followed:

$$\begin{bmatrix} D_1 \\ D_2 \\ D_3 \end{bmatrix} = \begin{bmatrix} d_{11} & d_{12} & d_{13} & d_{14} & d_{15} & d_{16} \\ d_{21} & d_{22} & d_{23} & d_{24} & d_{25} & d_{26} \\ d_{31} & d_{32} & d_{33} & d_{34} & d_{35} & d_{36} \end{bmatrix} \begin{bmatrix} T_1 \\ T_2 \\ T_3 \\ T_4 \\ T_5 \\ T_6 \end{bmatrix} + \begin{bmatrix} \varepsilon_{11}^S & \varepsilon_{12}^S & \varepsilon_{13}^S \\ \varepsilon_{21}^S & \varepsilon_{22}^S & \varepsilon_{23}^S \\ \varepsilon_{31}^S & \varepsilon_{32}^S & \varepsilon_{33}^S \end{bmatrix} \begin{bmatrix} E_1 \\ E_2 \\ E_3 \end{bmatrix} \quad (10)$$

$$\begin{bmatrix} S_1 \\ S_2 \\ S_3 \\ S_4 \\ S_5 \\ S_6 \end{bmatrix} = \begin{bmatrix} S_{11}^E & S_{12}^E & S_{13}^E & S_{14}^E & S_{15}^E & S_{16}^E \\ S_{21}^E & S_{22}^E & S_{23}^E & S_{24}^E & S_{25}^E & S_{26}^E \\ S_{31}^E & S_{32}^E & S_{33}^E & S_{34}^E & S_{35}^E & S_{36}^E \\ S_{41}^E & S_{42}^E & S_{43}^E & S_{44}^E & S_{45}^E & S_{46}^E \\ S_{51}^E & S_{52}^E & S_{53}^E & S_{54}^E & S_{55}^E & S_{56}^E \\ S_{61}^E & S_{62}^E & S_{63}^E & S_{64}^E & S_{65}^E & S_{66}^E \end{bmatrix} \begin{bmatrix} T_1 \\ T_2 \\ T_3 \\ T_4 \\ T_5 \\ T_6 \end{bmatrix} + \begin{bmatrix} d_{11} & d_{21} & d_{31} \\ d_{12} & d_{22} & d_{32} \\ d_{13} & d_{23} & d_{33} \\ d_{14} & d_{24} & d_{34} \\ d_{15} & d_{25} & d_{35} \\ d_{16} & d_{26} & d_{36} \end{bmatrix} \begin{bmatrix} E_1 \\ E_2 \\ E_3 \end{bmatrix} \quad (11)$$

Most piezoelectric materials are orthotropic; hence, the expanded matrices can be reduced to the following:

$$\begin{bmatrix} D_1 \\ D_2 \\ D_3 \end{bmatrix} = \begin{bmatrix} 0 & 0 & 0 & 0 & d_{15} & 0 \\ 0 & 0 & 0 & d_{24} & 0 & 0 \\ d_{31} & d_{32} & d_{33} & 0 & 0 & 0 \end{bmatrix} \begin{bmatrix} T_1 \\ T_2 \\ T_3 \\ T_4 \\ T_5 \\ T_6 \end{bmatrix} + \begin{bmatrix} \varepsilon_{11}^S & 0 & 0 \\ 0 & \varepsilon_{22}^S & 0 \\ 0 & 0 & \varepsilon_{33}^S \end{bmatrix} \begin{bmatrix} E_1 \\ E_2 \\ E_3 \end{bmatrix} \quad (12)$$

$$\begin{bmatrix} S_1 \\ S_2 \\ S_3 \\ S_4 \\ S_5 \\ S_6 \end{bmatrix} = \begin{bmatrix} S_{11}^E & S_{12}^E & S_{13}^E & 0 & 0 & 0 \\ S_{21}^E & S_{22}^E & S_{23}^E & 0 & 0 & 0 \\ S_{31}^E & S_{32}^E & S_{33}^E & 0 & 0 & 0 \\ 0 & 0 & 0 & S_{44}^E & 0 & 0 \\ 0 & 0 & 0 & 0 & S_{55}^E & 0 \\ 0 & 0 & 0 & 0 & 0 & S_{66}^E \end{bmatrix} \begin{bmatrix} T_1 \\ T_2 \\ T_3 \\ T_4 \\ T_5 \\ T_6 \end{bmatrix} + \begin{bmatrix} 0 & 0 & d_{31} \\ 0 & 0 & d_{32} \\ 0 & 0 & d_{33} \\ 0 & d_{24} & 0 \\ d_{15} & 0 & 0 \\ 0 & 0 & 0 \end{bmatrix} \begin{bmatrix} E_1 \\ E_2 \\ E_3 \end{bmatrix} \quad (13)$$

By the reversal of Kelvin-Voigt notation (Arnau & Soares, 2008), the elastic compliance tensor in Equation (13) can be converted to a four digits notation used in Abaqus (superscript E omitted) as shown as followed:

$$\begin{bmatrix} S_{11} & S_{12} & S_{13} & 0 & 0 & 0 \\ S_{21} & S_{22} & S_{23} & 0 & 0 & 0 \\ S_{31} & S_{32} & S_{33} & 0 & 0 & 0 \\ 0 & 0 & 0 & S_{44} & 0 & 0 \\ 0 & 0 & 0 & 0 & S_{55} & 0 \\ 0 & 0 & 0 & 0 & 0 & S_{66} \end{bmatrix} \rightarrow \begin{bmatrix} S_{1111} & S_{1122} & S_{1133} & 0 & 0 & 0 \\ S_{2211} & S_{2222} & S_{2233} & 0 & 0 & 0 \\ S_{3311} & S_{3322} & S_{3333} & 0 & 0 & 0 \\ 0 & 0 & 0 & S_{1212} & 0 & 0 \\ 0 & 0 & 0 & 0 & S_{1313} & 0 \\ 0 & 0 & 0 & 0 & 0 & S_{2323} \end{bmatrix} \quad (14)$$

Lastly, by performing a simple inverse of matrix, the elastic compliance tensor can be converted to an elastic modulus tensor that can be inputted into Abaqus for simulation purposes:

$$\begin{bmatrix} S_{1111} & S_{1122} & S_{1133} & 0 & 0 & 0 \\ S_{2211} & S_{2222} & S_{2233} & 0 & 0 & 0 \\ S_{3311} & S_{3322} & S_{3333} & 0 & 0 & 0 \\ 0 & 0 & 0 & S_{1212} & 0 & 0 \\ 0 & 0 & 0 & 0 & S_{1313} & 0 \\ 0 & 0 & 0 & 0 & 0 & S_{2323} \end{bmatrix} \rightarrow \begin{bmatrix} D_{1111} & D_{1122} & D_{1133} & 0 & 0 & 0 \\ & D_{2222} & D_{2233} & 0 & 0 & 0 \\ & & D_{3333} & 0 & 0 & 0 \\ & & & D_{1212} & 0 & 0 \\ & & & & D_{1313} & 0 \\ & & & & & D_{2323} \end{bmatrix} \quad (15)$$

2.4.2 Natural Frequency and Mode Shape

When a piezoelectric element is subjected to an external excitation, usually in the form of electrical excitation for converse piezoelectric effect, a strain will be induced. The magnitudes of this strain, and hence, displacement are very small relative to the required displacement for ultrasonic scalpels. Hence, ultrasonic transducers are usually designed to work at a resonant frequency which matches the mechanical vibration of the system where maximize displacement amplification of the piezoelectric element can be achieved. The resonant frequency of an ultrasonic transducer can have a specific mode shape (longitudinal, flexural or torsional), or a combination of 2 or more mode shapes. In Langevin transducers, the longitudinal mode shape is usually employed.

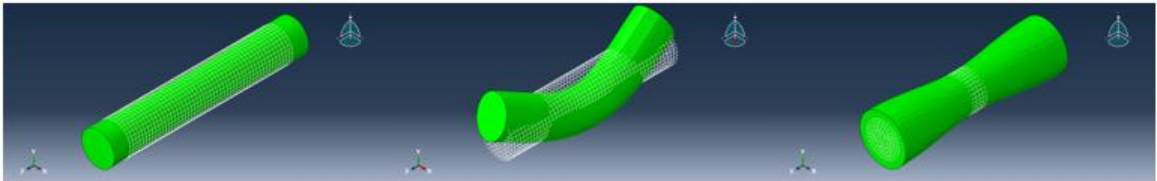


Figure 2.2: Longitudinal, flexural and torsional modes.

For obtaining the natural frequency of a system, a free-free end boundaries, fixed-free end boundaries and a fixed-fixed end boundaries scenarios can be performed. Ultrasonic transducers are usually simulated using the first case, where the system is assumed to free from any fixture, which can be approximated by tying a thin string to the transducer. The other two cases are normally utilized in piezoelectric energy-harvesting devices such as cantilever/bimorph beams clamped at one or both free ends (Wu & Chen, 2012). For all three cases, the system can be modelled as a simple mass-spring-damper system that is subjected to physical and vibrational working concepts such as damping, stiffness, forces, velocity etc. The following figure illustrates a simple equivalent mass-spring-damper system for a Langevin transducer:

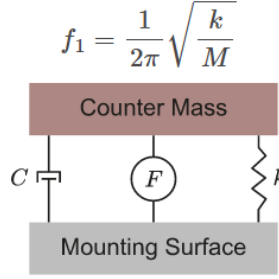


Figure 2.3: Simple lumped mechanical model for a Langevin transducer. (PiezoDrive, n.d.)

2.4.3 Electromechanical Coupling

The electromechanical coupling factor, k_{ij} indicates how well the system converts electrical input into mechanical output. The subscripts used, i and j used are similar to the one used in defining the piezoelectric charge constant, d , where the first subscript indicates the direction of input and the second subscript describes the direction of mechanical vibration developed. The value for piezoelectric materials is often provided by manufacturer as the theoretical maximum value of coupling factor. However, in actual application, electromechanical conversion is not as predicted due to nonlinearity effects and other forms of energy loss to the surrounding. Hence, the effective electromechanical coupling factor, k_{eff} can be calculated to represent the actual efficiency of energy conversion for a system, which can be calculated as followed (Berardengo et al., 2021):

$$k_{eff} = \sqrt{\frac{f_p^2 - f_s^2}{f_s^2}} \quad (16)$$

Where f_s and f_p are the resonant frequencies of the system under series and parallel configurations respectively.

2.4.4 Mechanical Quality Factor

The mechanical quality factor, Q_m , on the other hand, indicates the ratio of initial energy stored in the transducer to the energy loss in one radian of the oscillation. It is also the ratio of the reactance to the resistance in a series equivalent circuit representing an ultrasonic transducer system, which can be calculated as followed:

$$Q_m = \frac{1}{\omega_s C_1 R_1} = \omega_s L_1 R_1 = \frac{1}{4\pi C (f_a - f_r)} \quad (17)$$

Where,

- ω_s = Angular frequency
- C_1 = Equivalent capacity
- R_1 = Resonant resistance
- L_1 = Resonance inductance
- C = Capacitance
- f_a = Anti-resonance frequency
- f_r = Resonant frequency

An appropriate definition of mechanical quality factor related to amplitude in resonance is given by Shekani and Uchino such that it is an amplification factor of vibration of a piezo-resonator in resonance conditions (Shekhani & Uchino, 2015). The higher the magnitude of Q_m , the larger the resonant amplitude. The factor is also related to the loss factor as given below:

$$Q_m = \frac{1}{\tan \delta_m} \quad (18)$$

Similar to the electromechanical coupling factor, the mechanical quality factor for piezoelectric material is also commonly provided by the manufacturer.

2.4.5 Curie Temperature

The Curie temperature, or Curie point, is the temperature above which the material loses its piezoelectric properties (Mbarki et al., 2014). Hence, the piezoelectric material chosen for the design of ultrasonic transducer should have a sufficiently high Curie temperature since heat generation is prevalent in ultrasonic scalpel application.

2.5 Finite Element Modelling (FEM)

Due to rapid advancements of computer power and resources in the last couple of decades, designing an ultrasonic transducer has shifted gradually from analytical and experimental procedures to computer-aided simulation processes. The use of analytical models and experimental prototypes are inefficient comparatively. For analytical models, solutions of wave models are often complex and require excessive assumptions in which some are highly unrealistic. For experimental prototypes, the cost of fabricating a large

amount of prototypes are cost-intensive and the results are often non-reproducible (Al-Budairi, 2012). However, it is also irresponsible to assume that the prevalence of computer-aided simulations will totally replace analytical and experimental procedures as most FE platforms still rely on analytical framework for simulation procedures and experimental prototypes are still required for result validation. Nevertheless, FEM has since become a powerful tool in assisting designers and engineers to come out with products using minimized costs and accurate prediction of products' characteristics and properties.

According to Liu (2001), FEM is a method of predicting how a model of the actual product will react to external environmental factors such as forces, heat, electric field, pressure etc. It is a form of 'virtual prototyping' as the prototype may not be fabricated physically but property predictions can still take place. The core principle of FEM is to discretize the domain into finite number of smaller elements. By solving the related mathematical and physical formulations at these small elements, one can integrate the results of all small elements and predict the behaviour of the actual domain. Domains in FEM are generally regarded as a continuum and all points in space is continuous (Liu, 2001). The first commercial FEM software was initiated by MacNeal-Schwendler Corporation (MSC) in the form of NASTRAN (Engineering Software Research & Development Inc., n.d.). FEM software have since blossomed into a wide variety of platforms that includes SIMULIA Abaqus, ANSYS, and COMSOL Multiphysics etc.

Early contributions of Eer Nisse (1967) and Tiersten (1967) have established variation principles for piezoelectric media. In 1970, Allik and Hughes first formulated FE models for three-dimensional piezoelectric mediums in the form of tetrahedral volumetric element. In the following three decades, authors such as Lerch (1990), Tzou & Tseng (1990, 1991), Ha et al. (1992), Moetakef et al. (1995) and Lee & Saravanos (1996) had proposed piezoelectric analysis in other forms of model such as tetrahedrons, plane elements and beam elements (Piefort, 2001).

2.6 Longitudinal Vibration Mode and Langevin Transducer

The longitudinal vibration mode is the most common mode used for ultrasonic transducers (Predoi et al., 2014). Longitudinal mode of vibration is commonly employed

in Langevin transducers, where the vibrating piezoelectric material is sandwiched between metallic masses. Piezoceramics are used in most ultrasonic transducers, and when excited at the resonant frequency of the system, will produce longitudinal mode of vibration. The Langevin transducer design used for this project will be discussed in details in the next chapter.

The small displacement from the piezoelectric material is amplified through the ultrasonic horn with carefully-defined cross-sectional area variation. Various research papers have demonstrated different designs of ultrasonic horns with respective influence on the stress distribution and displacement amplitude. Rezaei et al (2021) developed an ultrasonic bone-cutting horn tool with a catenary longitudinal profile. The authors opined that the whole ultrasonic scalpel system should be analyzed together to ensure they all work at the same resonant frequency as they quoted most papers focused on the optimization of horn only. More complex horn profile such as the Bezier curve has also been investigated (Rai et al., 2020). The horn is generated using multi-objective optimization algorithm for cubic or quadratic curve, which can be observed in the works of Wang et al (2011), where a similar set of optimization algorithm was employed. The authors concluded that the new generation of Bezier horn is able to increase the amplitude magnification by 19% to 23.8% compared to conventional horn profiles.

2.7 Other Vibration Mode

Recently, attention of researchers in the field of ultrasonic transducer design have shifted from pure longitudinal vibration mode to other vibration modes such as torsional, flexional or combined mode. Research papers have discovered that by introducing certain geometrical features to the ultrasonic horn or resonator, the vibrational characteristics of these horns can be altered in favor of improving the ultrasonic transducer system performance. However, early designs and researches focused on industrial purposes such as machining, milling and cleaning, while those that are used for medical purposes were rare. Al-Budairi (2012) had formulated a detailed PhD thesis regarding the construction of a longitudinal-torsional horn used in piezoelectric transducers (Al-Budairi, 2012). An ultrasonic wiredrawing vibrator design utilized axially-poled single piezoelectric stack, which was different from the conventional ultrasonic vibrator driven by two or more

piezoelectricity stacks (Yang et al., 2015). An integrated ultrasonic variable amplitude system (IUVAS) utilizing longitudinal-torsional horn vibration mode was achieved by introducing helical slots on the conical section of the horn to achieve a combined vibration mode (Zhang et al., 2018). J. Li et al (2021) designed an advanced hemostatic ultrasonic scalpel using FEM and prototype fabrication with excellent cutting and coagulating capabilities proven by a coagulation dissection experiment. The shift from pure longitudinal mode to combined mode indicates a potential field of study for enhanced and improved ultrasonic transducer designs.

CHAPTER 3

RESEARCH METHODOLOGY

3.1 Overview

For this chapter, the research methodology applied throughout the project is discussed in details. For this project, the methodology is split into two distinct parts, which are the simulation part and experimental part. The subchapters of each part are summarized on the following chart.

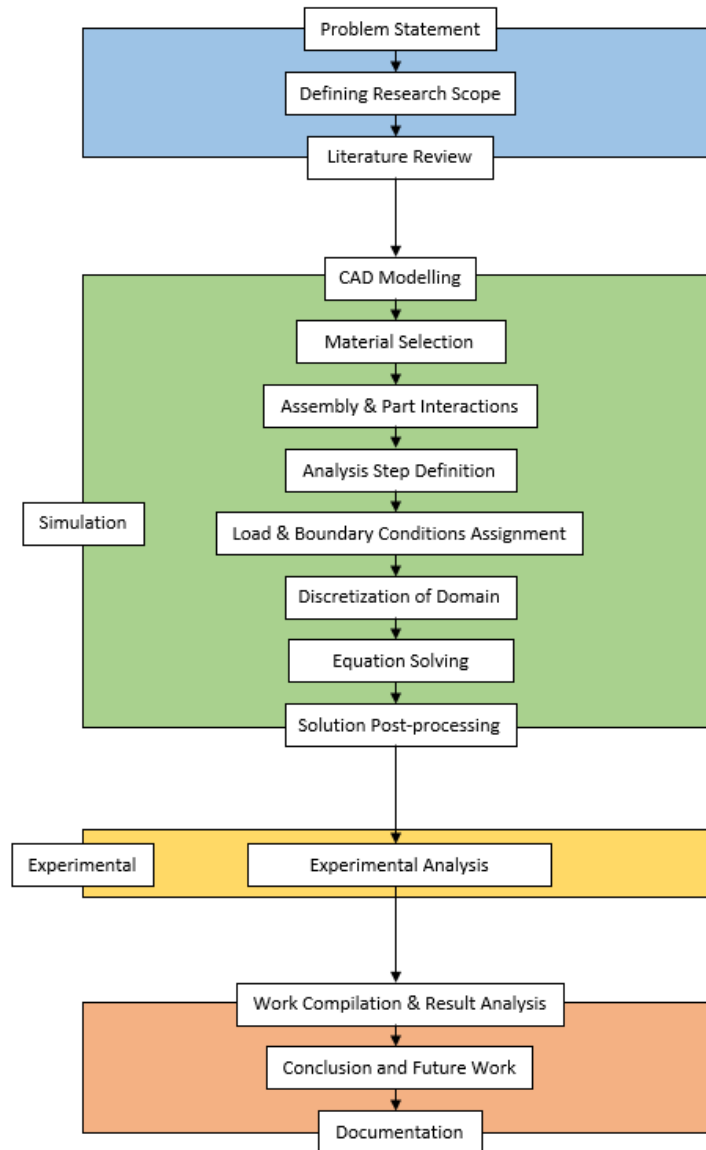


Figure 3.1: Overview diagram of solutions.

The simulation part acts as the prerequisite to the experimental part, and FEM is primarily used for simulating the ultrasonic transducer system's natural frequency, mode shape and harmonic response to an electrical excitation in the form of voltage function. The experimental part is conducted to characterize the existing prototype and to validate the simulation results in order to ensure the prototype performs as it is designed. The details of each element of both simulation and experimental parts will be explained in details in the following subchapters.

3.2 Simulation

In this subchapter, the details of the simulation process of the scalpel is explained in terms of the flow of simulation processes used in the FEM software Abaqus, from CAD Modelling to solution post-processing. The version of Abaqus used is Abaqus/CAE 2020. Abaqus is capable of finite element modelling in 1D, 2D and 3D modelling, in either a Standard Model or an Explicit Model. In this project, the Standard Model is used. Abaqus adopts a module-based structure, where there are 11 modules, in which nine of them will be used extensively for this project's simulation purposes. The modules used are:

- Part
- Property
- Assembly
- Step
- Interaction
- Load
- Mesh
- Job
- Visualization

Abaqus also allows the user to import CAD models created from other software as long as the part files are saved in a format readable by Abaqus, such as ACIS, STEP, IGES, and Parasolid etc. The simulation results from Abaqus is in the form of Output Database (ODB), and plots generated within the Visualization module can be exported to other graphing software such as MATLAB and Microsoft Excel.

3.3 CAD Modelling

The simulation process begins with CAD remodelling of the ultrasonic scalpel to produce the various parts used in the simulation. The existing ultrasonic scalpel is shown in Figure 3.2:

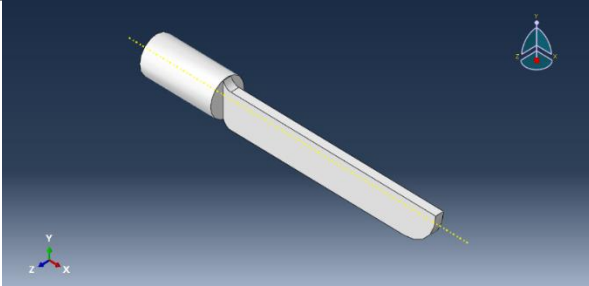
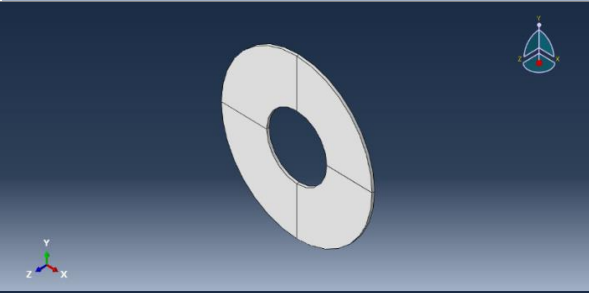
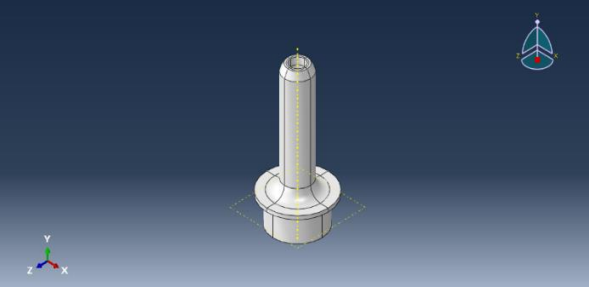
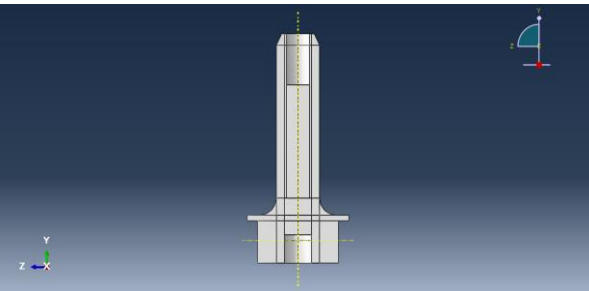
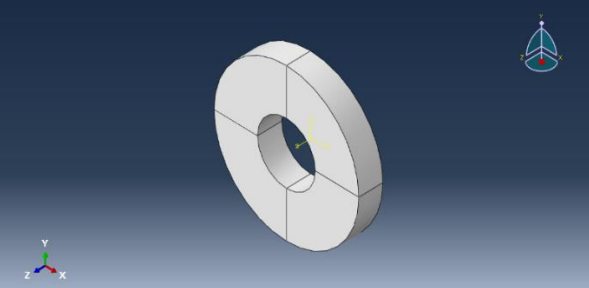


Figure 3.2: Existing ultrasonic scalpel.

The parts are drawn using the Part module in Abaqus. There are five distinct parts for this product, where each has its own dimensions and functions. Taking into consideration that there is no unit system utilized in Abaqus, apart from angle (in degree) and rotation (in radian), all dimensions used are self-consistent in the magnitude of meter (m). The Extrusion Base Feature is used to create the cutting tool, electrode and the piezoceramic ring, while the Revolution Base Feature is used for the back mass and front mass due to their axisymmetric geometry. The parts created are summarized in the following table:

Table 3.1: Parts and their functions.

Part	Function(s)	Image
Back mass	<ul style="list-style-type: none"> • Provides adequate preloading • Transfer vibration to the front mass 	

Part	Function(s)	Image
Cutting tool	<ul style="list-style-type: none"> • Cutting interface 	
Electrode	<ul style="list-style-type: none"> • Provides correct polarity to the rings 	
Front mass	<ul style="list-style-type: none"> • Acts as resonator to amplify vibrational amplitude from the rings 	  <p>(Sectional view along Y-Z plane)</p>
Piezoceramic ring	<ul style="list-style-type: none"> • Provides electromechanical conversion • Source of vibration for transducer system 	

Partitions are used in this section to divide the parts to allow better meshing, which will be explained in details in the Section: Discretization of Domain. Extrusions and